Systematic Prediction of Kinetically Limited Crystal Growth Morphologies

Danxu Du,[1] David J. Srolovitz,[1] Michael E. Coltrin,[2] and Christine C. Mitchell[2]
[1]Department of Mechanical and Aerospace Engineering, Princeton University, Princeton, New Jersey 08540, USA
[2]Sandia National Laboratories, P.O. Box 5800, Albuquerque, New Mexico 87185, USA
(Received 15 June 2005; published 5 October 2005)

We develop a new, combined experimental and theoretical approach to make reliable predictions for the limiting case of surface reaction kinetics controlled growth. We solve the inverse problem of determining the growth velocity from observations of the evolution of the morphology of GaN islands grown by metalorganic chemical vapor deposition and make use of crystal symmetry and established theorems. We are able to predict the growth for both convex and concave surfaces, with faceted and curved features. We also give a general guideline for deducing growth velocities from experimental observations.

DOI: 10.1103/PhysRevLett.95.155503 PACS numbers: 81.10.−h, 81.10.Aj, 81.15.Aa, 81.15.Gh

In chemical vapor deposition (CVD) and metalorganic CVD (MOCVD), crystal growth rates are determined largely by gas phase transport (unlike in evaporation growth or sputtering). If vapor-phase transport is sufficiently fast such that each section of the growth front is exposed to the same chemical environment, the evolution of the surface may be surface reaction limited. In this case, the evolution will be determined entirely by a single function—the surface orientation-dependent growth velocity. This can be expressed through a velocity plot (v plot) in which the length of the radius vector is proportional to the growth velocity and its orientation is that of the surface normal [1]. Unlike kinetically limited growth shapes, the equilibrium crystal shape can be determined by convexifying the plot of surface free energy, γ, versus surface normal (i.e., γ plot) [2,3]—this is equivalent to minimizing the total free energy with respect to the total surface free energy. Such a procedure leads to the well-known Wulff shape. Application of the Wulff construction to the v plot predicts the asymptotic growth shape in the kinetically controlled growth regime (i.e., the kinetic Wulff shape or idiomorph) [4,5]. Unfortunately, the full v plot is rarely known (since only the slowest-growing orientations are normally observed). Nevertheless, the asymptotic shape of fully faceted crystals can be predicted if the velocities of all of the facets are measured. However, knowledge of the facet velocities alone is insufficient to predict the evolving crystal shape before this asymptotic regime is reached. This evolution is where growth morphologies are the most interesting. Level-set [6] and other sharp interface methods (e.g., the crystalline method [7]) have been proposed to describe morphology based upon facet growth velocities. Such approaches necessarily invoke mathematical artifices in order to maintain numerical stability (e.g., adding arbitrary tangential velocities [6]). While enjoying some notable successes, they are necessarily limited by assumptions regarding the shape of the v plot, exhibit numerical instabilities in special cases (e.g., concave growth), and/or do not account for initiation of new facets [6,7]. An alternative approach to predicting morphology is to develop a physical model based upon the coupling of thermodynamic and kinetic frameworks, such as in time-dependent Ginsburg-Landau theories [8,9]. However, such approaches still present difficulties since the anisotropy of the physical properties that are input to such approaches (e.g., surface energies and reaction rates) is rarely known.

In this Letter, we solve the inverse problem of determining the v plot from observations of the evolution of the morphology of GaN islands grown by MOCVD. This work has three unique features: (1) the design of growth templates that provide information on surfaces not normally observed in the kinetic Wulff shape, (2) the development of a rigorous approach to determining the nature of all possible singularities in the v plot, and (3) the development of a robust simulation technique that can describe growth morphologies without depending on numerical artifices. The resultant method is capable of describing the evolution of concave and complex shapes and of fully or partially faceted shapes. The approach is easily generalizable to other material systems and can be used as the basis for morphology design.

The growth experiments were performed within the framework of selective area growth (SAG) [also known as epitaxial lateral overgrowth (ELO)] in which GaN was grown through a mask [10–12] that was lithographically patterned to produce crystal islands with both convex and concave features. An initial 1 μm layer of GaN was grown on a sapphire substrate and then coated with a 0.2 μm Si_3N_4 layer. Several different patterns containing convex and concave sections were etched through the mask, exposing the underlying GaN (the etching produces holes with near flat, vertical walls). Upon further MOCVD growth, GaN grows only on the exposed GaN regions, and not on the mask [11,12]. GaN growth proceeds first through the holes etched into the mask and then both vertically and laterally across the surface of the Si_3N_4 mask layer. Illustrative GaN growth from annular, ''U notch,'' and elongated hexagonal holes are shown in Figs. 1(a), 2(a), and 3(a). The mask patterns were designed so as to determine the essential features of the v plot, i.e., relative velocities of important surfaces and the nature of singular-

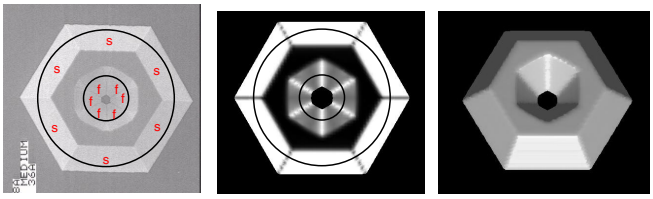

FIG. 1 (color online). (a) Experimental and (b),(c) simulated island shapes starting from a circular annulus pattern (inscribed). Panels (a) and (b) are plan views where the dark surfaces are {0001}; the very light and intermediate gray surfaces are the slow (s) $\{1\bar{1}01\}$ and fast (f) $\{11\bar{2}2\}$ orientations, respectively. An oblique view is shown in (c). The initial radius of the outer circle in the template is 10 μm and the height of the grown island in (a) is around 7 μm.

ities in the v plot (saddles, full and partial cusps). The discussion below shows how these singularities are systematically identified from the grown crystal shapes.

Figure 1 shows an island grown from a circular annular template. The island grows into a strongly faceted donut shape, the exterior and interior surfaces of which appear hexagonal in projection. Interestingly, the interior and exterior hexagons are rotated by 30° with respect to one another. The exterior surface is convex and is composed of $\{1\bar{1}01\}$ facets and the interior surface exposes only $\{11\bar{2}2\}$ facets separated by the top, flat (0001) facets. According to Herring [3], the presence of facets on convex surfaces implies the presence of cusps in the v plot in the direction normal to the facets. This implies the v plot has deep cusps in both the $\langle 1\bar{1}01\rangle$ and [0001] directions. Since these facets are part of surfaces that are convex in two directions: the in-plane φ direction [i.e., in the (0001) plane] and out-of-plane θ direction (angle measured relative to the [0001] direction), the cusps correspond to orientations where the surface growth velocity versus orientation has a discontinuity in slope in two directions (we refer to these as full cusps).

It is easy to show that for an inward growing (concave) surface, the growth morphology is dominated by facets for which the growth rate is a maximum in the v plot. For the annular template of Fig. 1, the "fast" facets are of the $\{11\bar{2}2\}$ type. However, the inward growing surface of the annular shape is not completely concave. It is concave in the in-plane φ direction, but convex in the out-of-plane θ direction; i.e., these are saddle surfaces. The presence of such a faceted saddle surface implies that the v plot has maxima with respect to the in-plane angle φ and a cusped minimum with respect to the out-of-plane angle θ in all of the $\langle 11\bar{2}2\rangle$ directions. The relative sizes of the $\{1\bar{1}01\}$, $\{11\bar{2}2\}$, and (0001) facets can be used to deduce the relative growth rates of these different facets: i.e., 1:3.8:8.5 based on the data in Fig. 1(a). (These specific growth ratios would change under different growth conditions, such as temperature, pressure, and NH_3:Ga ratio.)

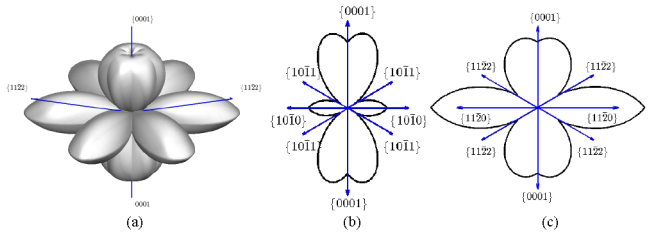

FIG. 2 (color online). The v plot: (a) a 3D view, (b) a $\{11\bar{2}0\}$ cross section, and (c) a $\{1\bar{1}00\}$ cross section.

Given the features of these 13 special orientations (we neglect growth down into the substrate), we can deduce the key features of the v plot. Unfortunately, the image in Fig. 1 does not provide absolute velocity information for any orientation other than these 13. To complete the v plot, we can interpolate between these special orientations (as long as they do not modify the kinetic Wulff shape). This lack of uniqueness is inherent in determining v plots from faceted structures.

There is one contradiction in the type of v plot described above. That is, the presence of sixfold symmetries is incompatible with the group symmetry of GaN. While GaN does not have a sixfold rotation axis, it does have a sixfold screw axis. The crystal morphology appears to be insensitive to the half-unit cell translation implied by the screw axis. However, since observations of the facets were made on a scale large compared with the unit cell, this translation information is lost. The symmetry of crystal growth is compatible with the group symmetry of the material after the removal of such translations (screw or glide translations). The space group minus the translations is known as the isogonal group (a term widely used in geology) [13].

Figure 2 shows a v plot that was deduced from knowledge of the behavior of the 13 special points (relative velocities and nature of the discontinuities in v) and is compatible with the isogonal group symmetry of GaN. Each of the curved surfaces is a trigonometric interpolation. While not unique, this v plot is compatible with all of these constraints. In order to verify that the resultant v plot is valid, we performed a series of simulations of GaN growth from the same template patterns as used in the experiments. This was done within the framework of the level-set method [14]. The level-set equations, together with the surface velocity description in Fig. 2, were numerically integrated on a regular grid using a third order Runge-Kutta method in time and a fifth-order weighted essentially nonoscillatory scheme in space [14]. The only physics in the simulations is the form of the v plot (Fig. 2). Unlike in other methods used to evolve faceted surfaces, no special-case algorithms or assumptions (other than the v plot itself) were used to keep facets flat and corners sharp or to limit which facets could appear.

The simulation results corresponding to the annular template are shown in Figs. 1(b) and 1(c). Comparison of these images with the experimental image in Fig. 1(a) demonstrates that the proposed v plot (and numerical

(a) (b) (c)

FIG. 3. (a) Experimental and (b),(c) simulated island shapes starting from a U-notch pattern (inscribed). In (a), the lower case black letters label orientations in the mask pattern and the white letters label facets on the as-grown island.

method) is capable of capturing the major features of the morphology of the growing island. The initially circular annular feature grows outward over the surface of the mask into a hexagonal convex surface and inwardly to form a hexagonal concave (saddle) surface. The interior shape is rotated from the outer one by 30°. The outer facets are of the $\{1\bar{1}01\}$ type and the inner are $\{11\bar{2}2\}$. Although the circular annular template of Fig. 1 initially has surfaces with all possible in-plane angles φ, the simulation shows that, as the surface evolves, the convex growth surfaces become dominated by the slow $\{1\bar{1}01\}$ orientations and the concave growth surfaces by the $\{11\bar{2}2\}$ orientations, in accord with the experiment. As seen in the perspective view [Fig. 1(c)], all facets are flat and meet at sharp edges (after a short growth period).

While it may not be a surprise that the v plot generated from measurements of the circular annulus is able to reproduce the correct growth morphology, a more severe test of the generality of the v plot is the ability to predict a range of growth morphologies to which it was not fitted. In order to make the test even more severe, we focus on patterns of lower symmetry. Figures 3 and 4 show SAG islands growing out of U notch and elongated hexagonal annulus etched patterns, respectively.

Figures 3(a)–3(c) show the scanning electron micrograph (SEM) of the U-notch island together with a plan and perspective view of the island shape predicted using the v plot of Fig. 2. The numerical simulation results show that the island exhibits $\{1\bar{1}01\}$ facets at the convex (outer) corners. This confirms the expectation that convex morphologies are dominated by the slow facets. The experimental results in Fig. 3(a) are consistent with this numerical simulations. Unlike in Fig. 1, however, the concave surfaces are continuously curved (not faceted) in the present case. This behavior is a consequence of the v-plot properties, deduced above. Focus first on the curved surfaces on the bottom left (labeled B) and right in Fig. 3(a). In the initial island shape, these regions are initially concave corners defined by two slow facets (as dictated by the template). The curved surface grows out from these corners faster than on the adjacent flat segments because the flat segments correspond to velocity minima, i.e., $\{1\bar{1}01\}$. Since the corner grows faster than the flat segments bounding it, the corner must round as it advances. Unlike in Fig. 1(a), where fast $\{11\bar{2}2\}$ facets form at concave corners, this is not possible here since there is only one possible fast $\{11\bar{2}2\}$ facet in the orientation range between the two slow $\{1\bar{1}01\}$ facets dictated by the template. On the other hand, the upper concave section of the template (labeled A) shows both curved surfaces and a sharp corner. On this part of the island surface, there are two fast $\{11\bar{2}2\}$ facets in the orientation range dictated by the template shape (the three slow $\{1\bar{1}01\}$ surfaces). Hence, two fast $\{11\bar{2}2\}$ facets form and meet at a sharp edge (seen as a vertical line below A). The curved surfaces smoothly meld the fast $\{11\bar{2}2\}$ facets into the template-dictated $\{1\bar{1}01\}$ facets. Hence, flat facets are seen on concave surfaces where at least two fast facet orientations (that are cusped saddle points in the v plot) are available. Both experimental and numerical results are consistent these observations. The generality of this observation has been confirmed by comparison with several other template shapes, not shown here. The differences between the concave surfaces in the upper and the lower sections of Fig. 3(a) illustrate that the shapes of concave surfaces are sensitive to the initial conditions until features grow to full maturity.

Figures 4(a)–4(c) show a SEM of the island growth from an elongated hexagonal annulus pattern, together with two images of the island shape predicted using the v plot of Fig. 2. The side flats and the surfaces that meet at the exterior corners are $\{1\bar{1}01\}$ facets. These exterior slow $\{1\bar{1}01\}$ flats and the corners are separated by fast $\{11\bar{2}2\}$ facets. These fast facets are remnants of the template shape and are growing to extinction as the island evolves. The interior of the elongated annulus is continuously curved, except near the tip, where the curves meet at a sharp angle. Measurement of this angle shows it is very close to 60° [in the projection shown in Fig. 4(b)], indicative of the sixfold isogonal symmetry of the crystal and the difference in the φ values of two $\{11\bar{2}2\}$ facets. These features are, again, in excellent agreement with the experimental observations as shown in Fig. 4(a). The excellent correspondence between the simulations and experiments not only shows the efficacy of the simulation procedure but also shows that the deduced velocity profile (v plot) is essentially correct. The main features of the v plot necessary to reproduce the GaN results are subtle: a sixfold symmetry about [0001], full cusps in both the θ and φ directions at the [0001] and

(a) (b) (c)

FIG. 4. (a) Experimental and (b),(c) simulated island shapes starting from an elongated hexagonal annulus pattern (inscribed).

$\langle 1\bar{1}01\rangle$ orientations, and the growth rate in the $\langle 11\bar{2}2\rangle$ directions corresponds to cusps only in the θ direction but a smooth maximum in the φ direction. Above all, the symmetry of the v plot should be that of the isogonal point group (C_{6v}^4) of the space group ($P6_3mc$) of GaN. Although there is no (0001) mirror in GaN, we simplified the numerical boundary conditions by assuming such a symmetry element (without loss of generality for [0001] GaN SAG). By correctly choosing these features in the v plot using the experimentally determined ratio of growth rates for the three facets types, we can describe all of the observed facets on both convex and concave surfaces, the continuously curved surfaces seen in the experiments, and the temporal evolution of the entire island morphology.

Both the simulations and experiments show an important, yet not widely appreciated, aspect of concave growth. If an initial shape has flat surfaces meeting at a corner, the corner will rapidly round during growth until a surface orientation corresponding to a velocity maximum occurs. If this velocity maximum is also a cusp (a cusped saddle in the v plot) in another direction, then both curved and flat surfaces result. If there are two such cusped saddle orientations between the orientations of the two initial flats, curved surfaces meeting along sharp edges will result.

General guidelines for deducing the basic features of the v plot from experimental observations are as follows. The symmetry of the v plot is that of the isogonal point group corresponding to the space group of the underlying crystal structure. If a stable facet appears on fully convex crystal surfaces, this orientation corresponds to a cusped minimum in the v plot in both θ and φ. Facets on fully concave crystal surfaces (not present with the templates employed) indicate maxima in the v plot both in the θ and φ directions. If the faceted crystal surface is convex in one direction and concave in another, this orientation corresponds to a cusped minimum in the convex direction and a maximum in the concave direction in the v plot; this is a cusped saddle point. If faceting is not observed (i.e., all surface orientations appear) on the convex or concave surfaces, the v plot is smoothly curved and standard procedures can be used to deduce its shape [7]. The present approach represents a general procedure for deducing the important features of the v plot from a small set of well-chosen templated growth experiments. The importance of using a reasonable description of the entire v plot for numerical modeling is not having to resort to artificial numerical procedures to maintain flat surfaces and sharp corners and to avoid numerical instabilities [6,7] and at the same time describe less important surfaces, not found in the kinetic Wulff shape.

In order to deduce the v plot from the selected area, growth experiments should contain several types of template shapes, for redundancy. Template shapes should contain both convex and concave features (such as the circular annulus). It is also useful to have template shapes that contain straight segments oriented parallel to the intersection of expected or possible facets with the substrate, such as those used here in Figs. 3 and 4 (this will, of course, depend upon crystal symmetry).

The approach discussed above, using experimental input to deduce a v plot, makes numerical simulation of complex growth geometries possible, such as for the case of patterned ELO growth of GaN or in other systems (e.g., see the interesting SAG of GaAs [15]). Such simulations will be an important quantitative tool to design complex SAG island structures for novel optoelectronic applications requiring pointed [16] or ridged [17] features, the presence of particular surface orientations, or in optimizing novel growth strategies. Following the experimental procedures, described above, permits the determination of v plots for any type of material and as a function of growth conditions using just one template mask and straightforward measurements in a SEM. Finally, by comparing the convex and concave growth surfaces, it is possible to determine whether observed growth morphologies are near equilibrium or kinetically controlled.

The authors thank Peter Smereka and Harris Wong for useful discussions. D. D. and D. J. S. acknowledge the support of the U.S. Department of Energy (Grant No. DE-FG02-99ER45797) and the Institute for Materials Research and Engineering, Singapore. The work at Sandia Laboratories was supported by the Office of Basic Energy Sciences, U.S. Department of Energy. Sandia National Laboratories is a multiprogram laboratory operated by Sandia Corporation, a Lockheed Martin Company, for the Department of Energy under Contract No. DE-AC04-94AL85000.

[1] J. Villain, Nature (London) **350**, 273 (1991).
[2] G. Wulff, Z. Krystallogr. Min. **34**, 449 (1901).
[3] C. Herring, Phys. Rev. **82**, 87 (1951).
[4] F. C. Frank, *Growth and Perfection of Crystals* (Wiley, New York, 1958).
[5] S. Osher and B. Merriman, Asian J. Math. **1**, 560 (1997).
[6] G. Russo and P. Smereka, SIAM J. Sci. Comput. **21**, 2073 (2000).
[7] J. E. Taylor, J. W. Cahn, and C. A. Handwerker, Acta Metall. Mater. **40**, 1443 (1992).
[8] J. W. Cahn and J. E. Hilliard, J. Chem. Phys. **28**, 258 (1958).
[9] S. M. Allen and J. W. Cahn, Acta Metall. **27**, 1085 (1979).
[10] R. Bhat, J. Cryst. Growth **120**, 362 (1992).
[11] C. C. Mitchell, M. E. Coltrin, and J. Han, J. Cryst. Growth **222**, 144 (2001).
[12] M. E. Coltrin and C. C. Mitchell, J. Cryst. Growth **261**, 30 (2004).
[13] C. Klein and C. S. Hurlbut, *The 22nd Edition of the Manual of Mineral Science* (J. Wiley, New York, 2002).
[14] S. Osher and R. P. Fedkiw, *Level Set Methods and Dynamic Implicit Surfaces* (Springer, New York, 2003).
[15] L. Jarlskog *et al.*, J. Cryst. Growth **222**, 534 (2001).
[16] B. L. Ward *et al.*, J. Appl. Phys. **84**, 5238 (1998).
[17] T. Sasaki, M. Kitamura, and I. Mito, J. Cryst. Growth **132**, 435 (1993).